17th Brazilian Congress of Thermal Sciences and Engineering
November 25th-28th, 2018, Águas de Lindóia, SP, Brazil

ENCIT-2018
THERMAL-HYDRAULIC EVALUATION OF THE AUGMENTATION OF HEAT TRANSFER IN A SOLAR WATER HEATER THROUGH LONGITUDINAL VORTEX GENERATOR

Felipe Augusto Santos da Silva
Sao Paulo State University (UNESP), Campus of Rosana, Energy Engineering, Av. Barrageiros, 1881, SP, 19274-000, Brazil.
fasantosdasilva@gmail.com
Leandro Oliveira Salviano
Sao Paulo State University, (UNESP), Department of Mechanical Engineering, Av. Brasil, 56, SP, 15385-000, Brazil.
leandro.salviano@unesp.br

Abstract. *The direct conversion of solar energy into thermal energy is an interesting alternative for heating a fluid. The use of the solar water heater can represent an average savings of electricity of up to 48% in some regions. Flat plate solar collector is used to transfer the solar energy for a working fluid. However, provide the increase of the heat transfer in such devices is remains as a great challenge. Longitudinal vortex generator for enhancement of the heat transfer is a passive technique which increases the amount of free movement into the boundary layer to provide a better mixture between the hot and cold streams near to the wall. This paper analyzes the application of the delta-winglet vortex generators for three different positions of an idealized plate in y-axis, which could be symmetrical or asymmetrical, for two different attack angles of 30° and 45°. The Reynolds number 600 and 900 were evaluated. The main result show that the delta-winglet vortex generator is an effective passive technique to provide heat transfer enhancement, resulting in 2.2 times the increase of heat transfer compared to the smooth tube, with pressure drop penalty of 4.4 times. The best ration between the heat transfer and the pressure drop penalty is reached for the attack angle of 30º and for the flat plate with eccentricity 0. Regarding to PEC, the best result is also obtained for the same setup of flat plate, for both attack angle of the vortex generators and for both Reynolds number.*

Keywords: *Thermal solar energy, Heat transfer enhancement, Passive technique, Delta-winglet vortex generators*

1. INTRODUCTION

The direct conversion of solar energy into thermal energy is an interesting alternative for heating of fluids in the domestic sector, industrial, tourism and hospitals (Jamar et al. 2016). In countries with high solar incidence, introducing solar water heating systems can represent an average savings of electricity of up to 48%, which can represent a reduction of up to 42% in the demand for electricity by a family of low income (Sowmy, Schiavon Ara, and Prado 2017). Flat plate solar water heater are devices that transfer the thermal energy solar into a fluid (Suman, Kaleem, and Pathak 2015). This type of solar collector consists of absorbing transparent cover plate, tubes, insulation and working fluid. The intensification of heat transfer in such devices remains as a great challenge and passive techniques could applied to increase the thermal efficiency (Garg et al. 2016).

The application of longitudinal vortex generators belongs to the class of passive techniques which are inserted inside of the tubes of the flat plate solar water heater, increasing the amount of free movement into the boundary layer and, consequently, the better mixture between the hot and cold fluid streams near to the wall (Lei et al. 2017).

In this way, the present work evaluated the increased heat transfer and the pressure drop penalty in a flat plate solar water heater through application of the delta-winglet longitudinal vortex generators. The attack angles of the longitudinal vortex generators at 30° and 45°, Reynolds numbers 600 and 900 and an idealized flat plate positioned in y-axis direction is evaluated.

2. COMPUTATIONAL METHODOLOGY

2.1 Governing equations

Numerical modeling of the heat transfer and fluid flow in a tube of circular cross-section is assumed to be a three-dimensional and incompressible flow, laminar and steady-state, (Cheshmeh 2012). For a Newtonian fluid with constant properties, the equations of Continuity, Momentum, and Energy are, respectively, as follow:

$$\frac{\partial}{\partial x_j}\left(\rho u_j\right) = 0 \tag{1}$$

$$\frac{\partial}{\partial x_j}\left(\rho u_j u_i - \tau_{ij}\right) = -\frac{\partial p}{\partial x_i} \tag{2}$$

$$\frac{\partial}{\partial x_j}\left(\rho u_j h - k\frac{\partial T}{\partial x_j}\right) = -u_j\frac{\partial p}{\partial x_j} + \tau_{ij}\frac{\partial u_i}{\partial x_j} \tag{3}$$

2.2 Thermal-hydraulic parameter

The flow in a circular tube is characterized by the Reynolds number and is calculated as a function of the tube diameter, Eq. (4). The parameters to perform the heat transfer and pressure loss are expressed by the Nusselt number and Friction factor, respectively, defined by Eq. (5) and Eq. (6).

$$Re = \frac{\rho u D}{\mu} \tag{4}$$

$$Nu = \frac{hD}{k} \tag{5}$$

$$f = \frac{2\Delta p}{\rho u^2}\frac{D}{L_T} \tag{6}$$

2.3 Computational domain and boundary conditions

Assuming a water uniform distribution through the tubes of the solar collector, the computational domain considers one tube, reducing the computational cost and, therefore, the solver time. An idealized plate of 980 mm of length and positioned at 10 mm from inlet at tube in the direction of the x-axis. Two configurations with ten longitudinal vortex generators placed on the top of the flat plate were evaluated. The flat plate is eccentrically positioned at 0.2R and 0.4R in y-axis direction, according to shown in Fig. 1. An another configuration considers the plat plate is positioned in the middle of the tube diameter (no eccentricity). For this last configuration, five longitudinal vortex generators were equally spaced on the top of the flat plate and five on the bottom side of the flat plate. The aspect ratio of the delta-winglet vortex generators is 2.

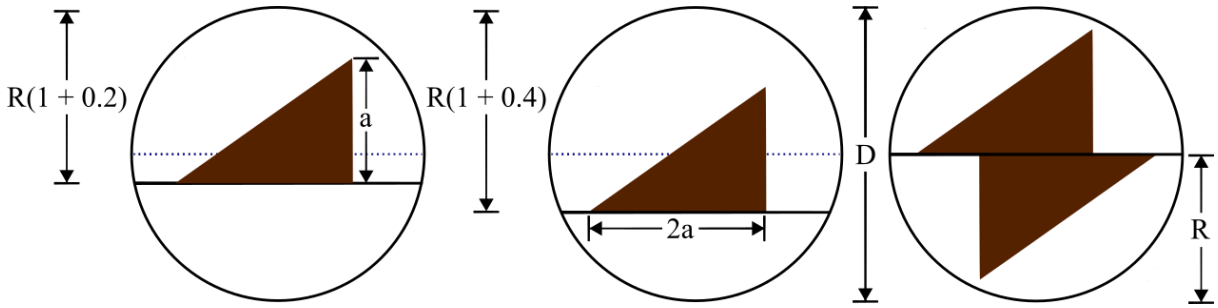

Figure 1. Transverse section of computational domain to show the position of the plate on the y-axis.

The attacks angles of the delta-winglet vortex generator of 30° and 45° were evaluated. A constant heat flux of 750 W/m^2 is set as the boundary condition on the tube surface, a uniform velocity is considered at inlet domain and an outlet pressure is fixed at the domain outlet. The conjugate heat transfer (conduction/convection) is solved for the Reynolds numbers of 600 and 900. Finally, no-slip condition on tube and vortex generators is assumed.

2.4 Grid independence and model validation

GCI methodology – Grid Convergence Index (Division et al. 2017), for mesh sensitivity analysis on three mesh densities is applied. The characteristics of each Grid are shown in Tab. 1.

Table 1. Characteristics of each Grid

Grids	Number of Elements	Refinement factor
Grid 1	574409	-
Grid 2	1248894	1.30
Grid 3	2777226	1.31

According to (Division et al. 2017), it is desirable that the Refinement Factor should be higher or equal than 1.30. Table 1 shows that this criterion is met in the present work. The GCI methodology is applied for the Reynolds number 900 and attack angle of the vortex generator of 45°, considering the flat plate at the middle of the tube diameter. The uncertainty due to mesh densities is 0.151% for the Nusselt number and 0.675% for the Friction factor. Thus, the grid independence is reached and the intermediate mesh (Grid 2) is chosen for the other numerical analysis.

Computational model validation is checked by comparison between the numerical simulation and theoretical values. According to (Incropera et al. 2014), the average Nusselt number for an internal flow under a laminar flow and full developed flow with constant heat flux on the surface is 4.36, while the Friction factor is 0.071, conform Eq. (7).

$$f = \frac{64}{Re} \tag{7}$$

It was considered the results of the Nusselt number and friction factor for the Reynolds number equal to 900 and internal flow in a smooth tube. The difference between the numerical and theoretical results for the Nusselt number and Friction factor are 3.54% and 2.54%, respectively. Therefore, these results indicate that the numerical approach adopted herein is reliable.

3. RESULTS AND DISCUSSION

A finite volume-based commercial software (ANSYS 18.2) to solve the governing equations was used. Figure 2 and Figure 3 show the increase of the Nusselt number and Friction Factor, respectively, for the tube with vortex generators in relation to smooth tube, for all Reynolds numbers, attack angles of the vortex generator and for configurations (eccentricity and no eccentricity).

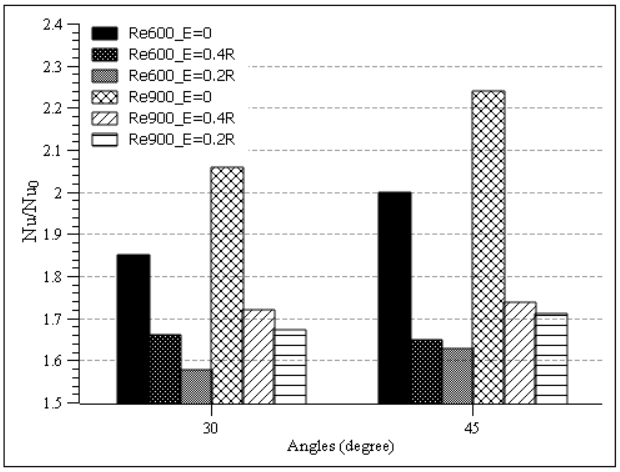

Figure 2. The increase of the average Nusselt number.

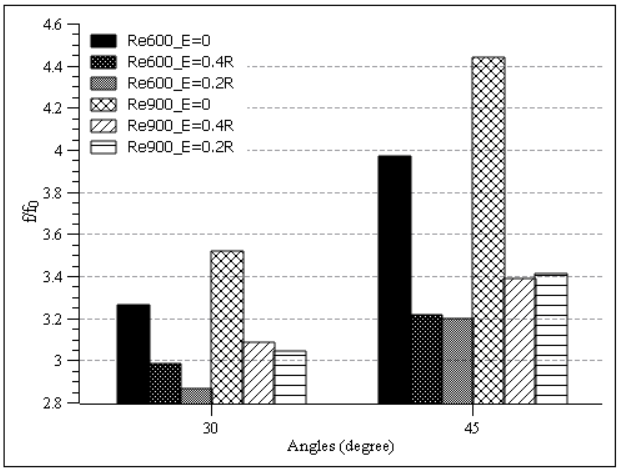

Figure 3. The increase of average Friction factor.

The highest Nusselt number ratio is observed for the tube with zero eccentricity, attack angle of the vortex generators equal to 45° and Reynolds number 900. The enhanced heat transfer is more than 2.2 times, Fig. 2, however, this configuration also presents the highest Friction factor ratio (4.5 times), Figure 3. Figure 2 and Fig. 3 also show that the increasing of attack angle increase the heat transfer with significant pressure drop penalty, and the eccentricity of 0.2R and 0.4R have similar results for both Reynolds number.

Figure 4 shows the ratio between the heat transfer and pressure drop penalty, which is compared to the Performance Evaluation Criteria (PEC) proposed by (Webb and Kim 2005), where the Friction factor is weighted for the exponent 1/3, in Figure 5. Than greater the reasons shown in Fig. 4 and in Fig. 5, better is the efficiency of the application of the delta-winglet longitudinal vortex generators.

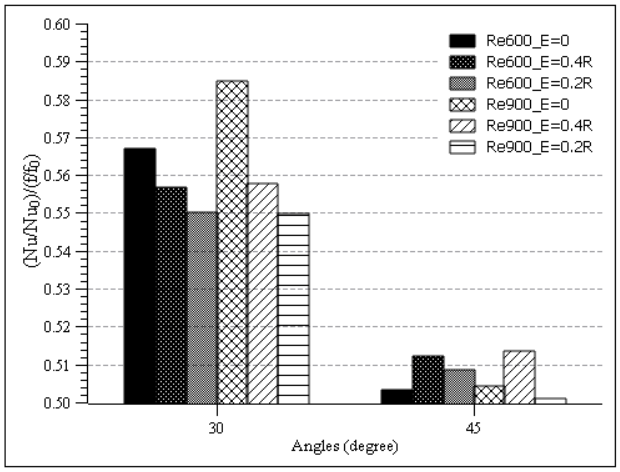

Figure 4. The ratio of the intensification of heat transfer with associated pressure loss.

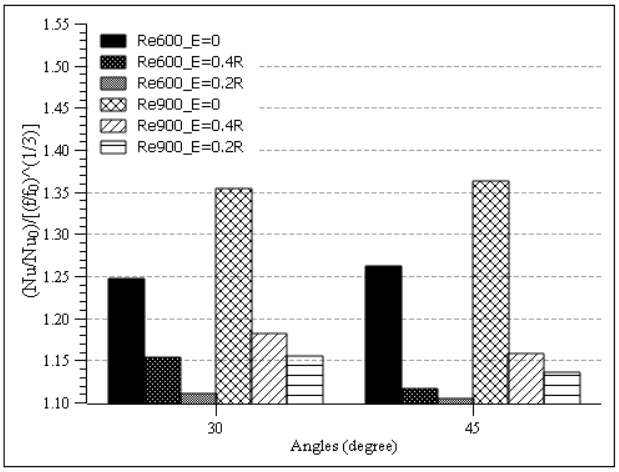

Figure 5. The ratio of the intensification of heat transfer with associated pressure loss according (Webb and Kim 2005).

In Fig. 4, the better results are observed for the tube with centralized flat plate with vortex generators at attack angle of 30° and Reynolds number at 900. Considering the E=0, the enhanced heat transfer at attack angle of 30º is 58% of the pressure drop penalty for Reynolds number 900 and 57% for Reynolds number 600. For models with vortex generators at attack angle of 45°, the intensification of heat transfer represents around 51% of the pressure drop penalty. Therefore, the best ratio between the heat transfer and the pressure drop penalty is reached for the attack angle of 30º and for the flat plate positioned in the middle of the tube diameter (E=0). Regarding PEC, Fig. 5, (Webb and Kim 2005), the best result is also obtained for the tube with the flat plate with eccentricity equal to 0, for both attack angle of the vortex generators and also for both Reynolds number. Different those results observed in Fig. 4, the PEC is quite similar for both attack angle for each configuration evaluated, which indicate that the PEC is quite independent of the attack angle. Overall, the attack angle of the vortex generators and the flat plate position are critical geometrical parameters to increase the solar water heater efficiency.

The flow dynamics for each configuration evaluated herein is analyzed through a CFD-Post software to visualize the streamlines tangential to the transverse planes at different positions along of the tube (x/L = 0.46, 0.51, 0.56 and 0.60), which represents the behavior of the fluid in the half of the computational domain (Tab. 2). The longitudinal and the transverse velocity profiles have also been evaluated in Tab. 3 and Tab. 4. Finally, the impact of the dynamic flow produced by longitudinal vortex generator on the temperature profile is shown in Tab. 5.

Table 2. Streamlines tangential to cross-cutting plans.

Attack Angle	Eccentricity 0							
	Re = 600				Re = 900			
	x/L				x/L			
	0.46	0.51	0.56	0.60	0.46	0.51	0.56	0.60
30º	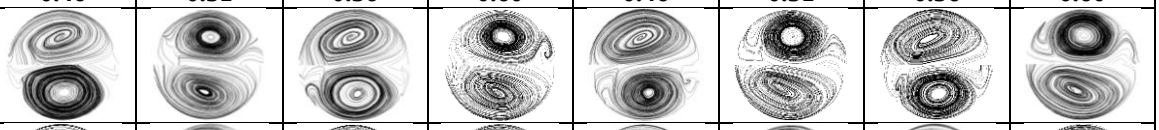							
45º	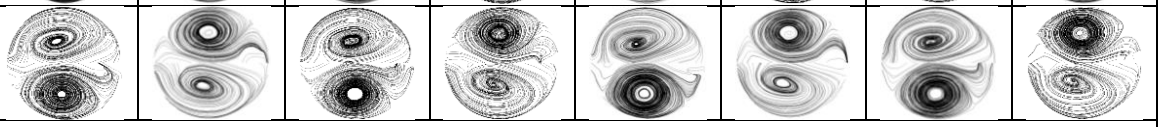							
Attack Angle	**Eccentricity 0.2R**							
	Re = 600				**Re = 900**			
	x/L				**x/L**			
	0.46	**0.51**	**0.56**	**0.60**	**0.46**	**0.51**	**0.56**	**0.60**
30º	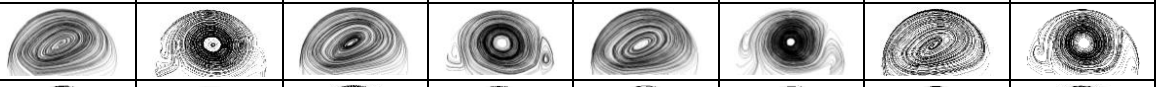							
45º	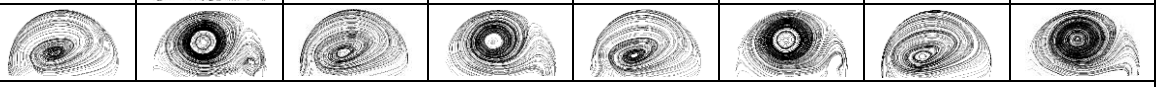							
Attack Angle	**Eccentricity 0.4R**							
	Re = 600				**Re = 900**			
	x/L				**x/L**			
	0.46	**0.51**	**0.56**	**0.60**	**0.46**	**0.51**	**0.56**	**0.60**
30º	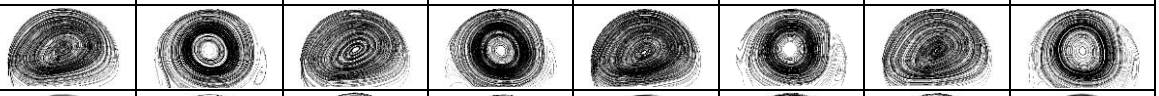							
45º	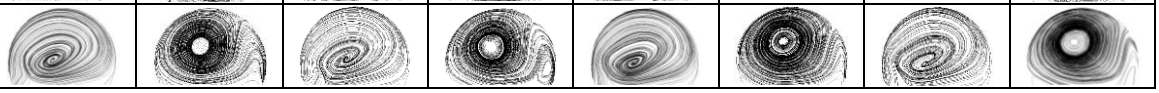							

Table 3. Velocity longitudinal profiles.

Without Vortex Generators	**Smooth**		
	Re = 600		
	0.46	**x/L**	**0.60**
	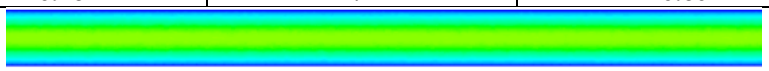		
	x/L		
	0.46	**Re = 900**	**0.60**
	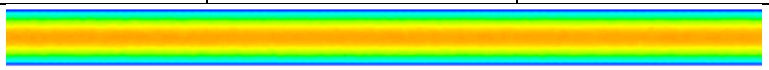		
Attack Angle	**Eccentricity 0**		
	Re = 600		
	0.46	**x/L**	**0.60**
30°	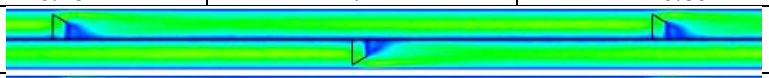		
45°	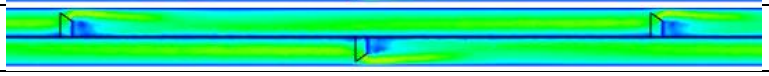		
Attack Angle	**Re = 900**		
	0.46	**x/L**	**0.60**
30°	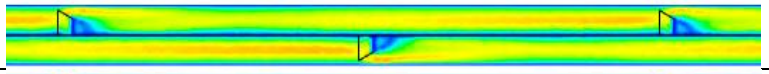		
45°	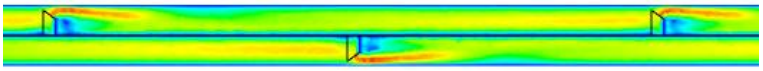		
Attack Angle	**Eccentricity 0.2R**		
	Re = 600		
	0.46	**x/L**	**0.60**
30°	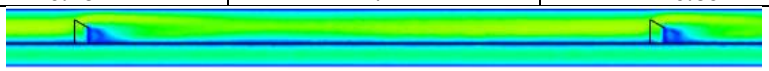		
45°	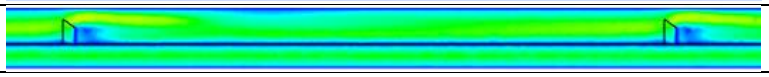		
Attack Angle	**Re = 900**		
	0.46	**x/L**	**0.60**
30°	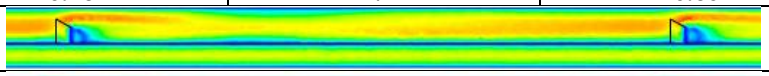		
45°	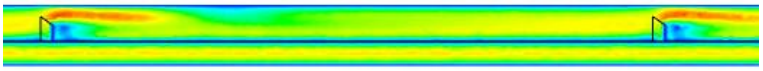		
Attack Angle	**Eccentricity 0.4R**		
	Re = 600		
	0.46	**x/L**	**0.60**
30º	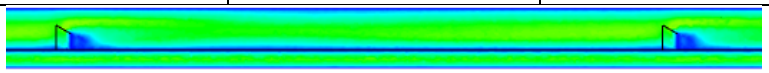		
45º	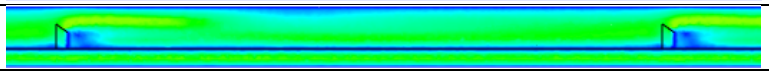		
Attack Angle	**Re = 900**		
	0.46	**x/L**	**0.60**
30º	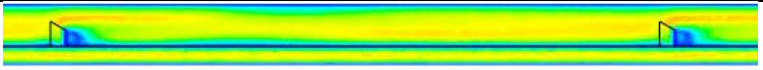		
45º	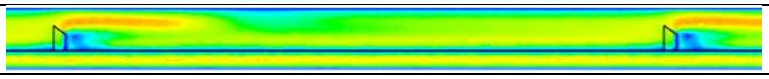		

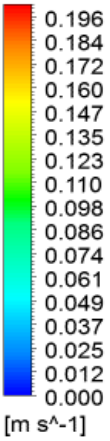

Table 4. Velocity profile at several cross-planes.

Without Vortex Generators	**Smooth**								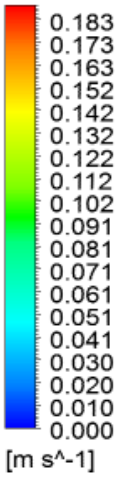
	Re = 600				**Re = 900**				
	x/L				**x/L**				
	0.46	**0.51**	**0.56**	**0.60**	**0.46**	**0.51**	**0.56**	**0.60**	
	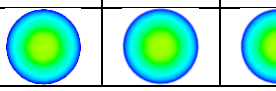								
Attack Angle	**Eccentricity 0**								
	Re = 600				**Re = 900**				
	x/L				**x/L**				
	0.46	**0.51**	**0.56**	**0.60**	**0.46**	**0.51**	**0.56**	**0.60**	
30º	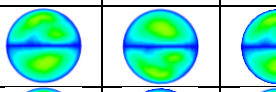								
45º	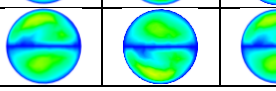								
Attack Angle	**Eccentricity 0.2R**								
	Re = 600				**Re = 900**				
	x/L				**x/L**				
	0.46	**0.51**	**0.56**	**0.60**	**0.46**	**0.51**	**0.56**	**0.60**	
30º	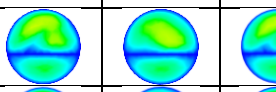								
45º	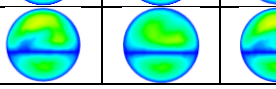								
Attack Angle	**Eccentricity 0.4R**								
	Re = 600				**Re = 900**				
	x/L				**x/L**				
	0.46	**0.51**	**0.56**	**0.60**	**0.46**	**0.51**	**0.56**	**0.60**	
30º	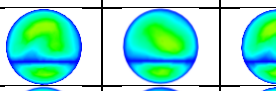								
45º	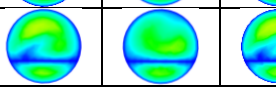								

Table 5. Temperature profile at several cross-planes.

Without Vortex Generators	**Smooth**							
	Reynolds 600				**Reynolds 900**			
	x/L				**x/L**			
	0.46	**0.51**	**0.56**	**0.60**	**0.46**	**0.51**	**0.56**	**0.60**
	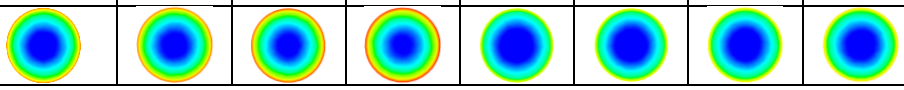							
Attack Angle	**Eccentricity 0**							
	Reynolds 600				**Reynolds 900**			
	x/L				**x/L**			
	0.46	**0.51**	**0.56**	**0.60**	**0.46**	**0.51**	**0.56**	**0.60**
30º	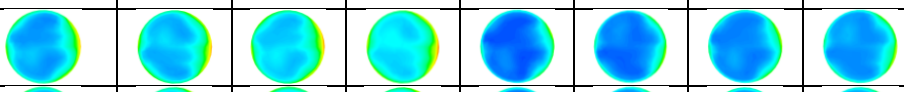							
45º	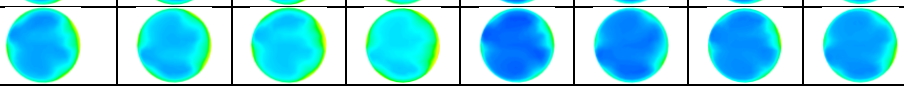							
Attack Angle	**Eccentricity 0.2R**							
	Reynolds 600				**Reynolds 900**			
	x/L				**x/L**			
	0.46	**0.51**	**0.56**	**0.60**	**0.46**	**0.51**	**0.56**	**0.60**
30º	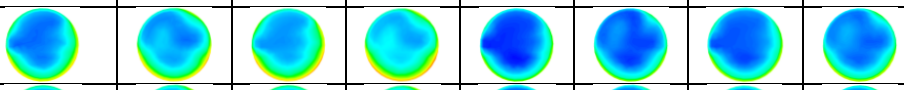							
45º	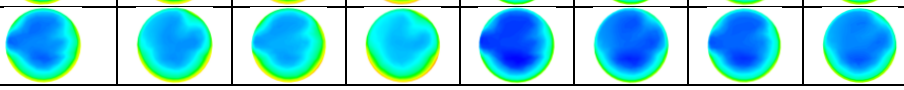							
Attack Angle	**Eccentricity 0.4R**							
	Reynolds 600				**Reynolds 900**			
	x/L				**x/L**			
	0.46	**0.51**	**0.56**	**0.60**	**0.46**	**0.51**	**0.56**	**0.60**
30º	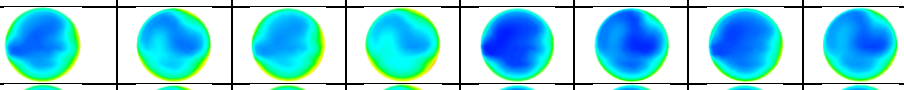							
45º	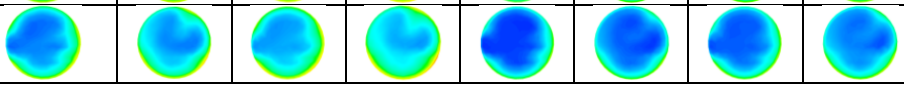							

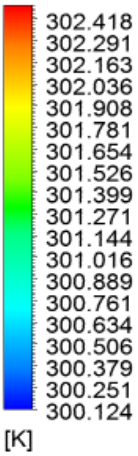

From Tab. 2 it is possible observes that the longitudinal vortex created at position x/L=0.46 is similar to vortexes at positions x/L=0.56, as well as the vortex at position x/L=0.51 are similar those at position x/L=0.60. This dynamic flow characteristic indicates that the flow behavior is periodical, for those all cases studied. In Tab. 3 low-velocity zones behind the insert can be observed, which contribute to increase the global pressure loss penalty on the system, although is very well knowledge that the strength of the longitudinal vortices is due to the local pressure difference between the frontal and back face of the vortex generator. These longitudinal vortex generators produced by inserts changing the flow dynamics inside the tube, that could be evaluated by comparison to smooth configuration which shown a parabolic profile.

Tab. 4 shows the velocity profiles at several positions along of the tube and the effect of the longitudinal vortices on flow could be verified. The longitudinal vortex generator accelerates the fluid and causes strong distortion on flow, which increase the mixture between the cold and hot streams of the flow. This conclusion could be corroborated evaluating the results present in Tab. 5. Moreover, the distortion of the flow due to vortex generator change the boundary layer growth which increase significantly the heat transfer and pressure drop penalty, according to show in Fig. 1 and Fig. 2.

4. CONCLUSIONS

In this paper, the application of the delta-winglet longitudinal vortex generators to the increase thermal conversion efficiency in a solar water heater is analyzed, which is solar devices inserts are usually applied in social residences through governmental actions. The performance of heat transfer and pressure drop penalty were numerically evaluated through commercial software ANSYS 18.2. The geometric parameters analyzed are: attack angle of the vortex generator (30° and 45º), position of an idealized flat plate in y-axis direction for Reynolds numbers at 600 and 900.

The major findings are summarized as follows:

- The application of delta-winglet vortex generator is an effective passive technique to enhance the heat transfer in a solar water heater;
- The geometric parameters evaluated are in fact critical to increase the thermal efficiency;
- The best results for the heat transfer enhancement is reached for the flat plate positioned in the middle of the tube diameter, E=0, for attack angle of 30º.
- In general, the eccentricity of 0.2R and 0.4R led to similar results;
- Performance Evaluation Criteria (PEC) is independent of the attack angle;
- The flow in the tube is periodical after the position x/L=0.41;
- The recirculation zone behind the vortex generator significantly contribute to global pressure drop penalty;

5. ACKNOWLEDGMENTS

The authors acknowledge the grants 2017/00608-0 and 2016/14620-9 of São Paulo Research Foundation (FAPESP) for the scientific initiation and fomentation, respectively. Acknowledge the São Paulo State University (Unesp), Campus of Rosana, for the infrastructure and academic support.

6. REFERENCES

Cheshmeh, Ali. 2012. “Velocity Boundary Layer Analysis of a Flat Plate Heat Exchanger in Laminar Flow : A Case Study” 2 (6): 310–14.

Division, Fluids Engineering, Editorial Policy Statement, Numerical Accuracy, Asme J Fluids Eng, Fluids Engineering, Editorial Policy, Numerical Accuracy, and Asme J Fluids Eng. 2017. “Procedure for Estimation and Reporting of Uncertainty Due to Discretization in CFD Applications” 130 (July 2008): 1–4. doi:10.1115/1.2960953.

Garg, M O, Himanshu Nautiyal, Sourabh Khurana, and M K Shukla. 2016. “Heat Transfer Augmentation Using Twisted Tape Inserts : A Review” 63. Elsevier: 193–225. doi:10.1016/j.rser.2016.04.051.

Incropera, Frank, David Dewitt, Theodore Bergman, and Adrienne Lavine. 2014. *Fundamentos de Transfêrencia de Calor E Massa*. Edited by LTC. 7thed.

Jamar, A, Z A A Majid, W H Azmi, M Norhafana, and A A Razak. 2016. “A Review of Water Heating System for Solar Energy Applications ☆.” *International Communications in Heat and Mass Transfer* 76. Elsevier Ltd: 178–87. doi:10.1016/j.icheatmasstransfer.2016.05.028.

Lei, Yonggang, Fang Zheng, Chongfang Song, and Yongkang Lyu. 2017. “Improving the Thermal Hydraulic Performance of a Circular Tube by Using Punched Delta-Winglet Vortex Generators.” *International Journal of Heat and Mass Transfer* 111: 299–311. doi:10.1016/j.ijheatmasstransfer.2017.03.101.

Sowmy, Daniel Setrak, Paulo Jos?? Schiavon Ara, and Racine T A Prado. 2017. “Uncertainties Associated with Solar Collector Efficiency Test Using an Artificial Solar Simulator.” *Renewable Energy* 108: 644–51. doi:10.1016/j.renene.2016.08.054.

Suman, Siddharth, Mohd Kaleem, and Manabendra Pathak. 2015. “Performance Enhancement of Solar Collectors — A Review.” *Renewable and Sustainable Energy Reviews* 49. Elsevier: 192–210. doi:10.1016/j.rser.2015.04.087.

Webb, Ralph L, and Nae-Hyun Kim. 2005. *Principles of Enhanced Heat Transfer*. Taylor & Francis.